ISSN 1022 - 2502, E-ISSN 2408- 8528
Dhaka Univ. J. Sci. 72(1): 63-70, 2024 (January) DOI: https://doi.org/10.3329/dujs.v72i1.71190

Preparation and Characterization of Porous Carbon Material from Banana Pseudo-Stem

Md. Mahmudur Rahman, Md. Enamul Kabir, Md. Mominul Islam, Md. Abu Bin Hasan Susan and Muhammed Shah Miran*

Department of Chemistry, University of Dhaka, Dhaka 1000, Bangladesh

(Received : 27 August 2023; Accepted : 13 December 2023)

Abstract

In this work, pseudo-stem of a banana plant was used as a sustainable and affordable source to prepare porous carbon materials (PCM) on a large scale. After fine treatment, the material was annealed at 500, 600, and 700 °C using a tube furnace under nitrogen flow. The prepared materials were characterized by Fourier transform infrared (FT-IR) spectroscopy, X-ray diffraction (XRD), scanning electron microscopy (SEM), transmission electron microscopy (TEM), and X-ray photoelectron spectroscopy (XPS). FT-IR spectra show that the broad peak at the range of 1110-1160 cm^{-1} comes from the superimposed peaks of C-N for a single or more than one functional group which debunks the possibility of generating nitrogen-doped carbon. TEM and SEM analyses confirmed the porous structure of PCM with the pores connected to one, and a spongy structure was observed in the prepared carbon material. XRD analysis revealed that the carbon materials are crystalline. XPS investigation provided information regarding the dimension of which elements are present in the valence states and constituent elements, depicting the presence of a dominant graphitic C1speak at approximately 284 eV, along with a distinct O1s peak at around 532 eV. Additionally, a relatively weaker N1s peak (approximately 400 eV) was observed.

Keywords: Banana pseudo-stem, activated carbon, porous carbon

I. Introduction

Carbon-based materials are the most abundant since they can occur in a variety of forms, including activated carbon (AC), graphene, carbon nanotubes, carbon dots, doped carbon, fullerenes, and others. However, dealing with carbon materials more often suffers from the drawbacks of the high expense and environmentally hostile nature. Carbon materials made from biomass have been produced and used since the dawn of civilization[1]. Over three thousand years ago, carbon black was produced from fuel-rich partial combustion to make ink, pigments, and tattoos[2]. The field of materials science focused on valuable carbon materials has experienced swift expansion following the identification of fullerenes and carbon nanotubes. This growth has been driven by the potential applications of these materials in areas such as fuel cells, electrodes, catalyst support structures, adsorption, gas storage, and carbon capture[3-9].

For the development of innovative synthetic materials possessing distinct structures and properties, nature provides an almost infinite source of ispiration[10-12]. Natural resources are nontoxic, accessible, plentiful, and sustainable. The natural products are composed of heteroatoms and could be used as an impactful and renewable source for functional carbons.

In recent studies, high-temperature carbonization and hydrothermal synthesis have been used to prepare the desired nanocarbon from biomass resources. Different carbonization processes have a key effect on particle size and surface morphology[13].AC has become a desirable alternative material due to its large specific surface area, inherent doping of heteroatoms, and economical nature[14]. A plenty of plant and animal bio-masses have been utilized for preparing advanced carbon materials[15]. The synthesis process has a significant impact on the structural and textural properties of AC. For the synthesis of AC, two main activation techniques—physical activation and chemical activation—are generally used[16]. Physical activation entails heating a precursor in a carbon dioxide (CO_2) or steam-reactive environment. Heating at a higher temperature (900-1000) °C is used to activate the residual char[17]. On the other hand, chemical activation entails coating precursors with a variety of chemical substances, including sodium hydroxide (NaOH), potassium hydroxide (KOH), sodium carbonate (Na_2CO_3), zinc chloride ($ZnCl_2$), phosphoric acid (H_3PO_4), nitric acid (HNO_3), magnesium chloride ($MgCl_2$), etc.[18-19]. The pyrolysis process of the initial materials is influenced by these chemical agents, which also serve as oxidizing and dehydrating agents. Carbon sequestration and aromatization have been used to prevent the loss of volatile substances and slow down the burning of initial materials, resulting in a significant increase in the production of various products[13-14]. A chemically activated approach is beneficial due to the creation of a large surface area, and uniform pore distribution[27].

In the case of a physically activated approach, the precursor should be pyrolyzed typically at a higher temperature to result in minimal production due to the loss of carbon as gases during heating. In order to produce AC with a high surface area and structural porosity, it may be beneficial to combine physical and chemical methods[15]. In light of this, a simple, cost-effective, and environmentally friendly method was developed for producing advanced carbon materials on a large scale using the pseudo-stem of the banana plant. The carbon materials were investigated by standard techniques

*Author for correspondence. e-mail: shahmiran@du.ac.bd

including Fourier transform infrared (FT-IR) spectroscopy, X-Ray diffraction (XRD), scanning electron microscopy (SEM), transmission electron microscopy (TEM), and X-ray photoelectron spectroscopy (XPS) in detail.

II. Experimental

Materials and Instruments

Chemicals

Banana pseudo-stem (*Musa ornata*) was collected from Barishal, Bangladesh. Analytical grade chemicals and materials such as sodium hydroxide, NaOH, sodium hydrogen carbonate, $NaHCO_3$(Merck, Germany), concentrated hydrochloric acid, HCl (RCI, Thailand), concentrated nitric acid, HNO_3 (Merck India), PVDF (Alfa Aesar, USA) were used without purification. De-ionized (DI) water (conductivity: 0.055 US cm^{-1} at 25 °C) from HPLC grade water purification systems (BOECO, BOE 8082060, Germany) was used throughout the study.

Synthesis of Materials

Preparation of porous carbon material (PCM) from banana pseudo-stem

The pseudo-stem of the banana was cut into small pieces and then cleaned with DI water. The clean pieces were dried for 24 h at 100 °C in an electric oven. The dried fragments were finely powdered using a regular household blender. Subsequently, this powder was passed through a 100-micron mesh sieve to achieve the desired particle size of less than 100 microns. After that, in a mortar achieved powder and $NaHCO_3$ were mixed with a mass ratio of 1:4. Then mixtures were carbonized at 500, 600, and 700 ^oC for 6 h using a tube furnace (Nabertherm, Germany) under nitrogen atmosphere. After carbonization, the final products were subjected to cleaning using 0.5 M HCl and DI water. Subsequently, they were dried overnight at 60 °C to yield porous carbon. The functionalized materials prepared in this manner were labeled as biomass-derived Carbon-700 (PCM-700), Carbon-600 (PCM-600), and Carbon-500 (PCM-500), all originating from banana pseudo-stems.

Characterization

TGA Analysis

A thermogravimetric analyzer (TG/DTA7200, HITACHI) was used for thermogravimetric analysis of the sample where the temperature limit was maintained between room temperature to 900 ^oC. In each case, a specific sample amount was placed in an alumina pan under a nitrogen environment. The sample was then heated at a rate of 10 °C per min.

FT-IR Spectroscopy

FT-IR spectra of the samples were recorded with Perkin Elmer FT-IR/NIR spectrometer (Frontier FTIR-NIR USA) in the range of 400-4000 cm^{-1} using KBr pellet prepared by mixing the sample with pure KBr; background correction was made with a pure KBr pellet to mitigate the influence of infrared active atmospheric gases such as carbon dioxide and water vapor in sample spectra.

SEM Analysis

A scanning electron microscope (SEM Model: JEOL, JSM-7600F, Japan) was employed to study the morphology of synthesized composites. The acceleration potential was 5kV with a probe current of 1.0 nA. Computer-adapted software ImageJ (1.51 k, Java 1.6.0-24 (64-bit), USA) was used to quantify the perimeter, total surface area, average particle size, and several nano-sized particles in the SEM images of synthesized composites at a defined scale.

TEM Analysis

A detailed internal structural analysis was carried out using a High-Resolution Transmission Electron Microscope (HRTEM) model (JEOL-JEM-1230, Tokyo, Japan). This microscope is equipped with a 200 kV field-emission electron gun operating in Schottky mode, enabling high-resolution imaging and analysis of subtle internal structures. For conducting TEM imaging, ethanol was used as a dispersion medium, and a small amount of the solid powder was sonicated for 1 min; after that, the solution was drop-casted on the carbon-coated copper grids. The TEM micrographs were analyzed by image analysis software (version 1.82.366, Gatan Inc. USA).

XRD Analysis

The X-ray diffraction pattern of the nanocomposites was recorded with PANalytical X'Pert Pro diffractometer operating at 40 KV and 30 mA using CuKα radiation (λ= 0.154056 nm) fitted with a scintillation detector. The sample was formed as powdered and then was put within two plain glass slides (25 nm × 75 nm).

XPS Analysis

The powder samples were first dispersed in ethanol and then applied onto a (1×1) cm^2 glass slide using the drop casting method. Afterward, the prepared slide was placed into the spectrometer for analysis. XPS spectra were acquired using a Thermo Fisher Scientific XPS spectrometer with an Alkα anode (energy 1486.68 eV) under pressure of 7×10^{-7} mbar. For survey scans, high-resolution elemental line scans were conducted at pass energy of 200 eV, while narrow scans of the hemispherical capacitor analyzer were performed at 50 eV pass energy. This yielded Ag 3d5/2 line with a full-width-at-half-maximum (FWHM) of less than 1

eV and intensity above a linear background from BE 365 eV to 371eV, with 1eV background averaging. An extra spectrum was obtained with a low pass energy of 3 eV to showcase the finest energy resolution of 0.5 eV. The energy scale of the spectrometer was aligned using the typical peak position of Cu2p3/2, Ag3d5/2, and Au4f7/2. Typically, the peak positions were within 50 meV of the standard peak energies. The binding energies of elemental lines were adjusted concerning the C 1s line of unintentional hydrocarbon contamination at binding energy (BE) of 284.8eV. High-resolution spectra (narrow scans) were captured for the Si2p, Ca2p, O1s, and C1s regions. The data analysis was carried out using Avantage1 software, with the additional point that curve fitting and deconvoluted data were both derived from this software.

III. Results and Discussion

Thermal Behavior

The TGA pattern for the banana pseudo-stem is shown in Fig. 1. It indicates the carbonization temperature for the banana pseudo-stem. Three steps of weight loss were observed in the TGA pattern (Fig. 1).

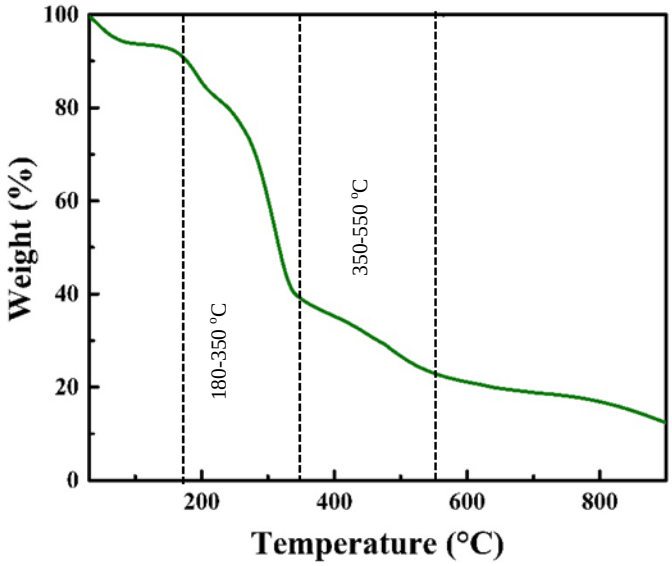

Fig. 1. TGA pattern for banana pseudo-stem.

TGA curve depicts a small weight loss at around 110 °C that may be with the virtue of the presence of traces of water or moisture in the pseudo stem. Volatile and non-volatile gases produced through decomposition are eliminated in the temperature range (180-350) °C. A sharp weight loss was noticed at 300 °C and it has been taken into account for carbonization of the pseudo stem. More than 70% weight loss occurs up to 550 °C and approaches to char phase. Fig. 1 also shows that the carbonaceous material remains stable at 800 °C. Therefore, the pseudo stem of banana plant has been pyrolyzed at 500, 600, and 700 °C.

Molecular Characterizations by FT-IR Spectral Analysis

The chemical structure and the functional groups in the synthesized material were first characterized by FT-IR spectroscopy as shown in Fig. 2. The FT-IR spectra of PCM materials confirmed some bands for functional groups involving carbon such as C-O (1050 cm^{-1}), C-H (1135 cm^{-1}), and C=C (1630 cm^{-1})[20]. The band at 1650 cm^{-1} and 1400 cm^{-1} in Fig. 2 indicates the presence of N-H bend for secondary amine and C-N stretching for aromatic tertiary amine, respectively[20]. Therefore, a C-N bond may be present. The other two bands in the fingerprint region are located between 800-600 cm^{-1}. A close resemblance exists between the PCM-600 and PCM-700 in Figure 2. The bands at 1430 cm^{-1} and 1630 cm^{-1} show the presence of C=C groups of aromatic compounds. While the presence of C-O-C of an ether group can be indicated by a bandat1050cm^{-1}. The bands at 500-600 cm^{-1} indicate the presence of a C-H group. The band at 2450 cm^{-1} of PCM-500 corresponds to the C-H stretch. These are comparable with other reported carbonaceous materials[40].

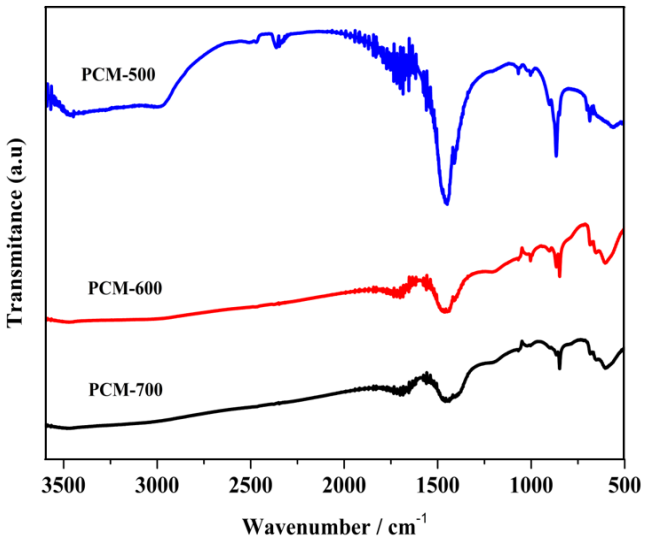

Fig. 2. FT-IR spectra of PCM-700, PCM-600, PCM-500.

Scanning Electron Microscopic Analysis

SEM analysis was conducted to study the surface morphology and microstructure of the prepared material. SEM was used to identify and quantify the number of particles of a specific size on the surface, thereby assessing the surface area characteristics of the material.Fig.3 shows different magnified SEM images of PCM-700 (a, b) and PCM-500 (c, d). Additionally, the SEM analysis revealed the presence of porous, three-dimensional (3D) frameworks comprising interconnected and distorted nanosheets. The external surface has a rough, uneven texture and little porosity. The SEM images of PCM-500 are shown in Fig. 3 (c, d), and it reveals that the material has been transformed into a porous carbon framework that resembles conventional activated carbon[21]. This suggests that $NaHCO_3$ could be an effective activating agent for the creation of porous structures. SEM images of PCM-700 (a, b) have provided visual evidence of an increase in pore size. This observation signifies the advancement of a porous structure, which facilitates efficient electrolyte transfer. Consequently, this development contributes to a favorable rate of performance[22]. The samples consist of a well-defined grain microstructure. Upon closer examination at high magnifications, the presence of distinct pores becomes evident in the image[23]. The material was found to possess a loose and porous structure, with interconnected elements held together by numerous pores. This arrangement resembled a spongy structure, implying the existence of a substantial specific surface area[24].

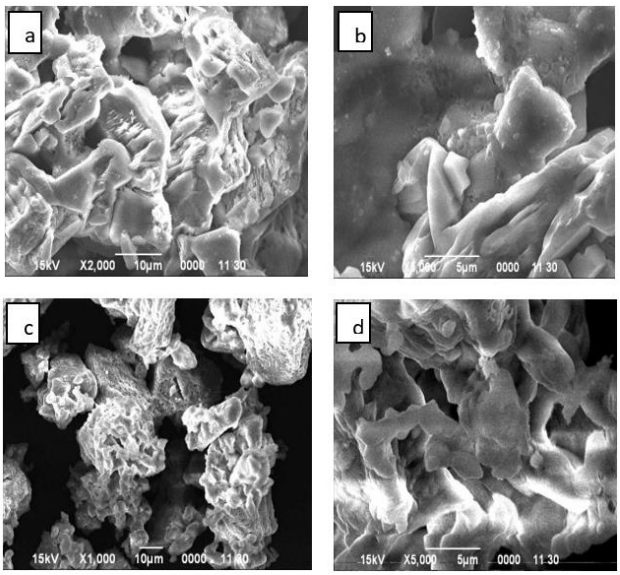

Fig. 3. SEM images of PCM-700 (a, b) and PCM-500 (c, d) at different magnifications.

The well-organized connections among these porous carbon nanosheets facilitate the rapid diffusion of electrolytes in applications involving electrochemical oxygen reduction reactions. The porous structure of the material could lead to enhanced ion transfer speed and improved electrolyte infiltration. Considering these advantages, the material holds the potential for effective electrode modification, making it a promising candidate for applications in supercapacitors[25].

Fig. 4 depicts the histogram of the particle size distribution for PCM-700 and PCM-500 samples determined from the FE-SEM images using Image J software, respectively. The smaller particles were found in PCM-700 compared to PCM-500. From the curve, the maximum sizes of particles for PCM-700 and PCM-500 were found within the ranges of 200-600 nm and 200-1000 nm, respectively. The average particle sizes of PCM-700 and PCM-500 are 480 and 644 nm.

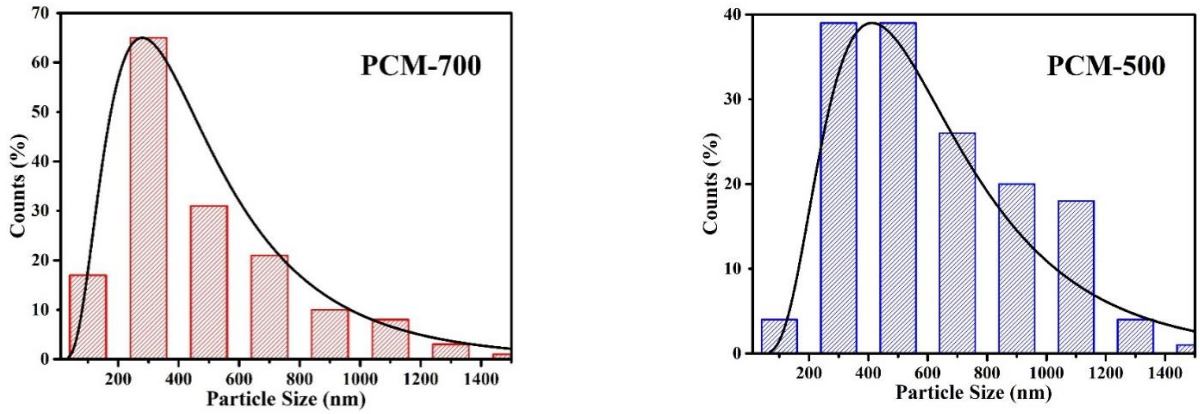

Fig. 4. Histogram showing particle size distribution determined SEM for PCM-700 and PCM-500 pure nanoparticles. Solid curves show estimated particle size distributions.

Transmission Electron Microscope Analysis

Fig. 5 shows the internal phase morphology of as-prepared carbon material. The PCM-600 sample exhibited a spongy and porous structure, along with a notably large specific surface area.

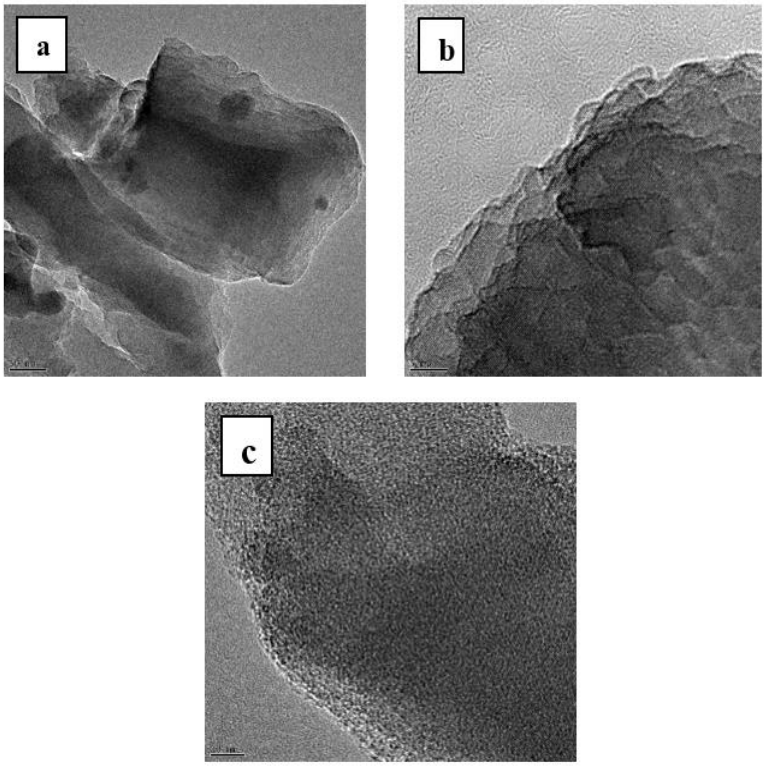

Fig. 5. TEM images (labeled as a, b, c) of PC-600 at different magnifications.

These features were prominently illustrated in panels (a, b, c). The spongy and porous structure, combined with the substantial specific surface area, plays a crucial role in enabling efficient mass and charge transfer during various electrochemical processes[26-27].

Degree of Crystallinity and Crystallite Size of Pyrolyzed Materials

X-ray diffraction analysis was conducted on the synthesized materials to confirm their crystalline nature. XRD patterns of PCM-700, PCM-600, and PCM-500 materials are shown in Fig. 6. A significant diffraction peak was observed within the 2θ range of 14 to 33°, which can be attributed to the characteristic activated carbon/crystalline carbon structure. This peak provides evidence of the crystalline properties of the materials[38]The presence of dominant peaks at 2θ values of 26.61°, 43.45°, 46.32°, 54.81°, and 56.68° corresponds to the (111), (100), (110), (222), and (211) orthorhombic crystal planes, respectively, as per the reference pattern JCPDS No. 083-2092. These peaks provide strong evidence of the crystalline nature. This material, derived from a pseudo stem, exhibits distinct crystallographic characteristics associated with these specific crystal planes.

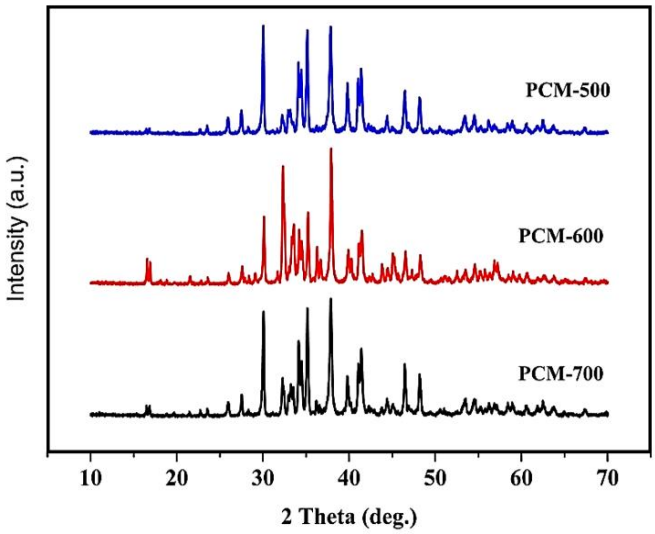

Fig. 6. XRD pattern of PCM-700, PCM-600, and PCM-500 materials.

In addition to the mentioned peaks, there are additional peaks observed at 2θ values of 15.13°, 23.186°, 24.16°, and 31.64°. These peaks correspond to the ($\bar{2}$02), ($\bar{1}$13), ($\bar{2}$13), and (021) monoclinic crystal planes. These additional peaks indicate the presence of a monoclinic crystal structure alongside the previously mentioned orthorhombic crystal planes. This suggests a more complex and diverse crystallographic composition in the synthesized carbon material derived from the pseudo stem[29]. Furthermore, the crystallinity of porous carbon increased from 80.83% for PCM-500 to 89.27% for PCM-700.

X-Ray Photoelectron Spectroscopy

XPS analysis was conducted to investigate the valence states and elemental compositions of the carbons. XPS survey spectra for PCM-700and PCM-500sample are shown in Fig. 6. From the survey spectra in Fig. 7, a predominant graphitic C1s peak at (ca. 284 eV) and a pronounced peak O1s peak at (ca. 532 eV), accompanied by a relatively weak N1s peak (ca. 400 eV), were observed in this Figure which depicts that activated carbon has been produced having nitrogen and oxygen-containing functionalities into the thermally treating biomass precursor. Furthermore, a trace amount of nitrogen atom is doped into the advanced activated carbon framework. Additional peaks were observed due to the presence of some minerals. The peak at ca. 500 eV might be due to V2p.

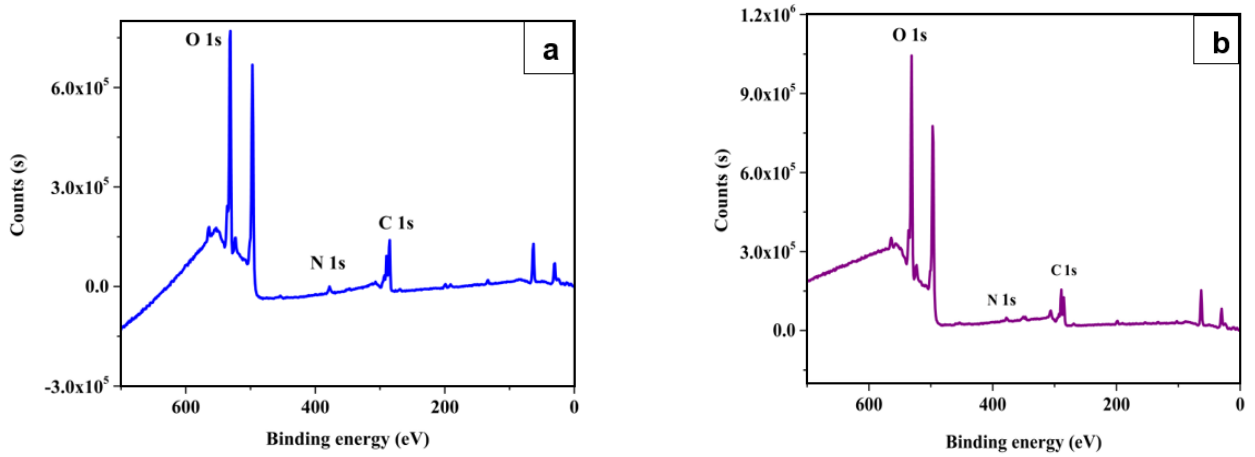

Fig. 7. XPS survey spectra for PCM-700 (a) and PCM-500 (b) sample.

IV. Conclusions

In this study, porous carbon materials were effectively synthesized using biomass, specifically banana pseudo-stems. The carbon materials were porous and had a spongy structure. The PCM-700, PCM-600, and PCM-500 showed the characteristics of activated crystalline carbon, notably highlighting the (110) and (202) lattice planes. A prominent C-N stretching band in FT-IR spectra suggested the incorporation of nitrogen, thus generating nitrogen-doped carbon. XPS analysis showed the presence of a dominant graphitic C1s peak at approximately 284 eV, along with a distinct O1s peak at around 532 eV. Additionally, a relatively weaker N1s peak (approximately 400 eV) was observed. The fundamental properties of prepared PCM show the prospect of being promising material for storing charge as supercapacitor and electrocatalyst that is underway in the laboratory.

Acknowledgment

Financial support for research projects from the Ministry of Science and Technology, Bangladesh and support from the University of Dhaka, Dhaka, Bangladesh are gratefully acknowledged.

References

1. Deb, A. K., M. S. Miran, M. Y. A. Mollah, 2013. Active carbon prepared from vegetable wastes for the treatment of Pb (II) in aqueous medium. *Bangladesh J. Sci. Ind. Res.*, **48(2)**, 97-104.

2. Suh, W. H., K. S. Suslick, G. D. Stucky, and Y. H. Suh, 2009. Nanotechnology, nanotoxicology, and neuroscience. *Prog. Neurobiol.*, **87(3)**, 133-170.

3. Kroto, H. W., J. R. Heath, S. C. O'Brien, R. F. Curl, and R.E. Smalley, 1985. C60: Buckminsterfullerene. *Nature*, **318(6042)**, 162-163.

4. Iijima, S., 1991. Helical microtubules of graphitic carbon. *Nature*, **354(6348)**, 56-58.

5. Sun, Y., C. Li, Y. Xu, H. Bai, Z. Yao, and G. Shi,2010. Chemically converted graphene as substrate for immobilizing and enhancing the activity of a polymeric catalyst. *Chem. Commun.*, **46(26)**, 4740-4742.

6. Titirici, M. M., A. Thomas, and M. Antonietti, 2007. Replication and coating of silica templates by hydrothermal carbonization. *Adv. Funct. Mater.*, **17(6)**,1010-1018.

7. Gong, K., F. Du, Z. Xia, M. Durstock, and L. Dai, 2009. Nitrogen-doped carbon nanotube arrays with high electrocatalytic activity for oxygen reduction. *Science*, **323(5915)**, 760-764.

8. Liu, R., D. Wu, X. Feng, and K. Müllen,2010. Nitrogen-doped ordered mesoporous graphitic arrays with high electrocatalytic activity for oxygen reduction. *Angew. Chem. Int. Ed.*, **49(14)**, 2565-2569.

9. Liu, D., X. Zhang, Z. Sun, and T. You, 2013. Free-standing nitrogen-doped carbon nanofiber films as highly efficient electrocatalysts for oxygen reduction. *Nanoscale*, **5(20)**, 9528-9531.

10. Parker, A. R., R. C. McPhedran, D. R. McKenzie, L. C. Botten, N.A.P. Nicorovici, 2001. Aphrodite's iridescence. *Nature*, 409(6816), 36-37.

11. Jeong, K.H., J. Kim, L. P. Lee, 2006. Biologically inspired artificial compound eyes. *Science*, **312(5773)**, 557-561.

12. Wang, K., H. Wang, S. Ji, H. Feng, V. Linkov, R. Wang,2013. Biomass-derived activated carbon as high-performance non-precious electrocatalyst for oxygen reduction. *RSC Adv.*, **3(30)**, 12039-12042.

13. Wang, K., Y. Jin, S. Sun, Y. Huang, J. Peng, J. Luo, J. Han, 2017. Low-cost and high-performance hard carbon anode materials for sodium-ion batteries. *ACS Omega*, **2(4)**, 1687-1695.

14. Ma, Q., Y. Yu, M. Sindoro, A. G. Fane, R. Wang, and H. Zhang, 2017. Carbon-based functional materials derived from waste for water remediation and energy storage. *Adv. Mater.*, **29(13)**, 1605361.

15. Köse, K. Ö., Pişkin, B., Aydınol, M. K., 2018. Chemical and structural optimization of $ZnCl_2$ activated carbons via high

temperature CO_2 treatment for EDLC applications. *Int. J. Hydrog. Energy*, *43*(40), 18607-18616.

16. Tyagi, A., S. Banerjee, S. Singh, and K. K. Kar, 2020. Biowaste derived activated carbon electrocatalyst for oxygen reduction reaction: Effect of chemical activation. *Int. J. Hydrog. Energy*, **45(34)**, 16930-16943.

17. Budinova, T., E. Ekinci, F. Yardim, A. Grimm, E. Björnbom, V. Minkova, and M. Goranova,2006. Characterization and application of activated carbon produced by H_3PO_4 and water vapor activation. *Fuel Process. Technol.*, **87(10)**, 899-905.

18. Li, W. H., Q. Y. Yue, B. Y. Gao, Z. H. Ma, Y. J. Li, and H. X. Zhao, 2011. Preparation and utilization of sludge-based activated carbon for the adsorption of dyes from aqueous solutions. *Chem. Eng. J.*, **171(1)**, 320-327.

19. Alonso-Lemus, I.L., B. Escobar-Morales, D. Lardizabal-Gutierrez, L.de la Torre-Saenz, P. Quintana-Owen, and F. J. Rodriguez-Varela, 2019. Onion skin waste-derived biocarbon as alternative non-noble metal electrocatalyst towards ORR in alkaline media. *Int. J. Hydrog. Energy*, **44(24)**, 12409-12414.

20. Duan, J., Y. Zheng, S. Chen, Y. Tang, M. Jaroniec, and S. Qiao,2013. Mesoporous hybrid material composed of Mn_3O_4 nanoparticles on nitrogen-doped graphene for highly efficient oxygen reduction reaction. *Chem. Commun.*, **49(70)**, 7705-7707.

21. Rahman, H. A., and S. X. Chin,2019. Physical and chemical properties of the rice straw activated carbon produced from carbonization and KOH activation processes. *Sains Malays.*, **48(2)**, 385-391.

22. Wang, Y., C. Shao, S. Qiu, Y. Zhu, M. Qin, Y. Meng, and L. Sun, 2019. Nitrogen-doped porous carbon derived from ginkgo leaves with remarkable supercapacitance performance. *Diam. Relat. Mater.* 98, 107475.

23. Maher, M., S. Hassan, K. Shoueir, B. Yousif, and M. E. A. Abo-Elsoud,2021. Activated carbon electrode with promising specific capacitance based on potassium bromide redox additive electrolyte for supercapacitor application. *J. Mater. Res. Technol.*, 11, 1232-1244.

24. Liu, X., Y. Zhou, W. Zhou, L. Li, S. Huang, and S. Chen,2015. Biomass-derived nitrogen self-doped porous carbon as effective metal-free catalysts for oxygen reduction reaction. *Nanoscale*, **7(14)**, 6136-6142.

25. Sun, Y., J. Xue, S. Dong, Y. Zhang, Y. An, B. Ding, and X. Zhang, 2020. Biomass-derived porous carbon electrodes for high-performance supercapacitors. *J. Mater. Sci.*, **55**, 5166-5176.

26. Liu, X., Zhou, Y., Zhou, W., Li, L., Huang, S., Chen, S., 2015. Biomass-derived nitrogen self-doped porous carbon as effective metal-free catalysts for oxygen reduction reaction. *Nanoscale*, ***7*(14)**, 6136-6142.

27. Zhang, S., M. S. Miran, A. Ikoma, K. Dokko, and M. Watanabe, 2014. Protic ionic liquids and salts as versatile carbon precursors. *J. Am. Chem. Soc.*, **136(5)**, 1690-1693.

28. Khalil, H. P. S., M. Jawaid, P. Firoozian, U. Rashid, A. Islam, and H.M. Akil, 2013. Activated carbon from various agricultural wastes by chemical activation with KOH: preparation and characterization. *J. Biobased Mater. Bioen.*, **7(6)**, 708-714.

29. Sofyan, N., S. Alfaruq, A. Zulfia, and A. Subhan, 2018. Characteristics of vanadium doped and bamboo activated carbon coated $LiFePO_4$ and its performance for lithium ion battery cathode. *J. Kim. Kemasan*, **40(1)**, 9-16.